

## Activation of protease calpain by oxidized and glycated LDL increases the degradation of endothelial nitric oxide synthase

Yunzhou Dong, Yong Wu, Mingyuan Wu, Shuangxi Wang, Junhua Zhang, Zhonglin Xie, Jian Xu, Ping Song, Kenneth Wilson, Zhengxing Zhao, Timothy Lyons, Ming-Hui Zou\*

Harold Hamm Oklahoma Diabetes Center and Section of Diabetes and Endocrinology, Department of Medicine, University of Oklahoma Health Sciences Center, Oklahoma City, OK, USA

Received: April 30, 2008; Accepted: June 16, 2008

### Abstract

Oxidation and glycation of low-density lipoprotein (LDL) promote vascular injury in diabetes; however, the mechanisms underlying this effect remain poorly defined. The present study was conducted to determine the effects of 'heavily oxidized' glycated LDL (HOG-LDL) on endothelial nitric oxide synthase (eNOS) function. Exposure of bovine aortic endothelial cells with HOG-LDL reduced eNOS protein levels in a concentration- and time-dependent manner, without altering eNOS mRNA levels. Reduced eNOS protein levels were accompanied by an increase in intracellular  $Ca^{2+}$ , augmented production of reactive oxygen species (ROS) and induction of  $Ca^{2+}$ -dependent calpain activity. Neither eNOS reduction nor any of these other effects were observed in cells exposed to native LDL. Reduction of intracellular  $Ca^{2+}$  levels abolished eNOS reduction by HOG-LDL, as did pharmacological or genetic through calcium channel blockers or calcium chelator BAPTA or inhibition of NAD(P)H oxidase (with apocynin) or inhibition of calpain (calpain 1-specific siRNA). Consistent with these results, HOG-LDL impaired acetylcholine-induced endothelium-dependent vasorelaxation of isolated mouse aortas, and pharmacological inhibition of calpain prevented this effect. HOG-LDL may impair endothelial function by inducing calpain-mediated eNOS degradation in a ROS- and  $Ca^{2+}$ -dependent manner.

**Keywords:** calcium homeostasis • calpain activation • endothelium dysfunction • eNOS, heavily oxidized and glycated-LDL (HOG-LDL) • nitric oxide

### Introduction

Metabolic syndrome and type 2 diabetes are insulin-resistant states that are commonly associated with atherogenic dyslipidaemia involving mild to moderate elevation of triglycerides, low levels of high-density lipoprotein cholesterol (HDL-C) and a preponderance of small dense low-density lipoprotein (LDL) [1]. Elevated LDL is a classical risk factor for atherosclerotic cardiovascular disease. In diabetes, elevation of LDL is exacerbated by qualitative modifications, including glycation and oxidation. Native LDL (N-LDL), which is found in the plasma of

healthy individuals, becomes glycated (glycated LDL) in the plasma of diabetic patients. After extravasation and prolonged entrapment in the arterial sub-intimal space, this glycated LDL may become severely oxidized [2], and in the present work this form of modified (*i.e.* glycated, then oxidized) LDL is represented by an *in vitro* preparation of 'heavily oxidized' glycated LDL (HOG-LDL). The pro-inflammatory and pro-atherogenic effects of oxidized LDL as well as the close involvement of modified form of LDL in the initiation and progression of atherosclerosis are well established [3]. In diabetes, hyperglycaemia increases not only glycation but also oxidative stress, resulting in oxidation of proteins, lipids and DNA or modification of these macromolecules with covalent adducts [4, 5]. Glycation of LDL slows the clearance of the particles from the blood circulation [6] increases the susceptibility of particles to oxidative damage [7], enhances entrapment of extravasated particles in the sub-intimal space and increases chemotactic activity of monocytes [8]. For these reasons, glycation of LDL is intimately connected with the formation of oxidized LDL.

\*Correspondence to: Ming-Hui ZOU, M.D., Ph.D., Harold Hamm Oklahoma Diabetes Center and Section of Diabetes and Endocrinology, Department of Medicine, University of Oklahoma Health Sciences Center, BSEB 325, 941 Stanton L. Young Blvd., Oklahoma City, OK 73104, USA.  
Tel.: 405-271-3974  
Fax: 405-271-3973  
E-mail: ming-hui-zou@ouhsc.edu

Injury to vascular endothelial cells is implicated in atherosclerosis and thrombosis [9]. Under normal conditions, endothelial nitric oxide synthase (eNOS) generates the vasoprotective molecule, nitric oxide [9, 10]. Vascular nitric oxide has a variety of functions, the most important being dilation of all types of blood vessels to maintain vascular homeostasis [10]. In atherosclerosis, a reduction in eNOS-derived nitric oxide impairs endothelium-dependent relaxation, with this impairment occurring before vascular structural changes arise [11]. Type 2 diabetes is associated not only with oxidant stress and accelerated endothelial apoptosis, but also with impaired endothelium-dependent relaxation [12, 13]. Indeed, endothelial dysfunction characterized by reduced nitric oxide bioactivity is a critical component of accelerated atherosclerosis associated with type 2 diabetes. Both hyperglycaemia and dyslipoproteinemia have also been implicated in the acceleration of diabetic vascular complications.

Oxidized LDL promotes endothelial cell toxicity and vasoconstriction both *in vitro* and *in vivo*. Plasma levels of oxidized LDL correlate with endothelial dysfunction and are reduced following lipid-lowering therapy using apheresis or statins (reviewed by Navab *et al.* [14]). Plasma levels of oxidized LDL were also recently shown to be an independent determinant of coronary macrovasomotor and microvasomotor responses elicited by bradykinin in human beings [15]. Circulating levels of oxidized LDL have been proposed to be a predictor of secondary cardiovascular events [16]. However, the molecular mechanisms by which HOG-LDL impairs endothelial dysfunction are poorly understood. Thus, the aim of the present study was to determine the effects of HOG-LDL on eNOS function by isolating LDL from healthy donors and then modifying it *in vitro*. Here, we demonstrate that HOG-LDL triggers endothelial dysfunction *via* Ca<sup>2+</sup>-mediated, calpain-dependent eNOS degradation.

## Materials and methods

### Materials

MDL 28170 (carbobenzoxy-valinyl-phenylalaninal) was purchased from Calbiochem (Gibbstown, NJ, USA). Other calpain inhibitors (ALLN, ALLM, calpeptin and E-64) and the fluorescent calpain substrate, Suc-leu-Leu-Val-Tyr-AMC, were obtained from BioMol International (Plymouth Meeting, PA, USA). The Fluo-4 NW calcium assay kits, dihydroethidium (DHE) and 2',7'-dichlorofluorescein (DCF) were obtained from Invitrogen (Carlsbad, CA, USA). Antibodies against eNOS, phospho-Ser1177 of eNOS and 3-nitrotyrosine-specific antibody were obtained from Cell Signaling Technology (Danvers, MA, USA). Calpain 1 antibody, calpain 1-specific siRNA and scrambled siRNA were purchased from Santa Cruz Biotechnology, Inc. (Santa Cruz, CA, USA). Recombinant eNOS and 4, 5-diaminofluorescein (DAF-2) were obtained from Cayman Chemical (Ann Arbor, MI, USA). Calcium channel blockers (CoCl<sub>2</sub>, LaCl<sub>3</sub>, Verapamil), diphenyleneiodonium chloride (DPI) and 4'-hydroxy-3'-methoxyacetophenone (apocynin) were purchased from Sigma-Aldrich (St. Louis, MO, USA). All other chemicals were from Fisher Scientific (Pittsburgh, PA, USA) and were of the highest available grade.

### Animals

C57BL/6J mice aged 10 weeks were obtained from the Jackson Laboratory (Bar Harbor, ME, USA). Mice were housed in temperature-controlled cages under a 12-hr light/dark cycle and were given free access to water and food. The animal protocol was reviewed and approved by the Institutional Animal Care and Use Committee at the University of Oklahoma Health Sciences Center.

### Preparation of N-LDL and HOG-LDL

The isolation of LDL from human donors was approved by the Institutional Review Board at the University of Oklahoma Health Science Center. Both N-LDL and HOG-LDL were prepared as previously described [17].

### Cell culture and treatment

Bovine aortic endothelial cells (BAECs) at passage 10 were cultured in endothelial basal medium (EBM; Lonza, Walkersville, MD, USA) containing 2% fetal bovine serum (FBS). Confluent BAECs were treated with the indicated concentration of HOG-LDL for varying times. When required, BAECs were exposed to BAPTA-AM (1,2-bis-[o-Aminophenoxy]-ethane-N,N,N',N'-tetraacetic acid, tetraacetoxymethyl ester), EGTA, calpain inhibitors, Ca<sup>2+</sup> channel blockers and NADPH oxidase inhibitors for 0.5–1 hr prior to the addition of HOG-LDL. BAECs treated with N-LDL (100 µg/ml, which is believed to be the physiological concentration) served as controls.

### Measurement of eNOS dimers/monomers

Levels of eNOS dimers/monomers were assayed using low-temperature SDS-PAGE, without boiling samples, as previously described [18].

### Immunocytochemical staining of eNOS and calpain 1

Calpain 1 and eNOS immunostaining was performed as described elsewhere [19]. Briefly, BAECs were cultured on cover slips and fixed with 4% paraformaldehyde. After blocking, BAECs were incubated with a mouse anti-eNOS antibody (BD Transduction Laboratories, San Jose CA, USA), or rabbit anti-calpain 1 antibody overnight at 4°C. Cell and tissue sections were then incubated for 30 min. at room temperature with biotinylated antimouse or anti-rabbit IgG secondary antibodies. The slides were rinsed, incubated with Fluorescein Avidin D (Vector Laboratories, Burlingame, CA, USA) for 30 min., counterstained with 4',6-diamidino-2-phenylindole (DAPI), mounted in Vectashield™ mounting media (Vector Laboratories) and viewed on a SLM 510 laser scanning confocal microscope (CARL Zeiss Meditec, Inc., Jena, Germany).

### Measurement of reactive oxygen species

Reactive oxygen species (ROS) were assayed using DHE (for superoxide [O<sub>2</sub><sup>-</sup>]) and DCF (for hydrogen peroxide [H<sub>2</sub>O<sub>2</sub>]) fluorescent dyes as described previously [18, 20].

## Reverse transcription and real-time quantitative PCR (qPCR)

After treatment with N-LDL or HOG-LDL, BAECs were repeatedly washed and total RNA was extracted (RNeasy Mini Kit, Qiagen, Valencia, CA, USA). RNA concentrations were determined using the NanoDrop<sup>®</sup> ND-1000 UV-Vis Spectrophotometer. Reverse transcription was performed with 1 µg of total RNA using the ThermoScript RT-PCR System (Invitrogen, cat# 11146-024), according to the manufacturer's protocol. SYBR Green real-time PCR primers used for amplification of bovine eNOS (GeneBank Access No. M99057) and bovine GAPDH (GeneBank Access No. NP\_001029206) were as follows: eNOS, forward 5'-TACCAGCCGGGGGACCACATAGGC-3', reverse 5'-CTCCAGCTGCTCCACAGCCACAGAC-3'; GAPDH, forward 5'-GCAGACGGTGCAGCGCATCTTGG-3', reverse 5'-TGGGTACGTATACGGCTTGTCAC-3'. qPCR was performed on 2 µl/well of reverse-transcribed product (20 ng total RNA) using the iQ TM SYBR<sup>®</sup> Green Supermix kit (Bio-Rad, Hercules, CA, USA, cat# 170-8882). The qPCR mixture was heated to 95°C for 3 min. and then subjected to 40 cycles at 95°C for 30 sec., 57°C for 30 sec. and 72°C for 1 min. using the MyiQTM System (Bio-Rad). The cycle threshold (Ct) value was determined for each sample. All Ct values were normalized to the internal control gene GAPDH ( $\Delta Ct = C_{\text{target}} - C_{\text{control}}$ ). The relative expression of eNOS mRNA, as determined by Ct value, was calculated using the equation,  $2^{-\Delta Ct}$  [21].

## Measurement of intracellular calcium

Intracellular Ca<sup>2+</sup> concentration was measured using the Fluo-4 NW kit, according to the instruction from the manufacturer, and the relative fluorescent units of intracellular calcium was expressed as fold induction over control.

## Measurement of calpain activity

Calpain activity assays were performed with a previously described method with minor modification [22]. Briefly, culture medium was aspirated from N-LDL or HOG-LDL-treated BAECs, and cells were washed with Hepes buffer (Invitrogen, pH 7.4). Cells were then incubated with Suc-leu-Leu-Val-Tyr-AMC in Hepes buffer for 30 min., and fluorescence was recorded (Ex: 360 ± 20 nm, Em: 460 ± 20 nm). Calpain activation was confirmed by monitoring cleavage of the calpain substrate, caspase-12, by Western blot.

## Measurement of 26S proteasome activity

The 26S proteasome activity was assayed using the fluorogenic proteasome substrate, Suc-LLVY-7-amido-4-methylcoumarin, as detailed previously [23].

## Transfection of calpain 1-specific siRNA

After serum deprivation for 24 hrs, confluent human umbilical vein endothelial cells (HUVECs) were transfected with calpain 1-specific siRNA

or scrambled siRNA according to the manufacturer's instructions. Forty-eight hours later, HUVECs were lysed for Western blot analysis of calpain 1 and eNOS.

## Measurement of nitric oxide

BAECs were cultured in EBM medium overnight in 24-well plates and incubated in N- or HOG-LDL for an additional 6 hrs. Cells were then incubated in phenol red-free EBM medium containing 2.5 µM DAF-2 for 30 min. in a CO<sub>2</sub> incubator. Nitric oxide levels were determined by measuring fluorescence (Ex/Em: 495/515 nm) and were expressed as a percentage of fluorescence emitted by control cultures.

## Measurement of endothelium-dependent and -independent vasorelaxation

Aortas were isolated from mice, cut into 3-mm rings and mounted in organ chambers (PowerLab, AD Instruments, CO, USA) in Krebs's buffer. After a 60-min. equilibration, rings were exposed to N-LDL or HOG-LDL (100 µg/ml each) in the absence or presence of the calpain inhibitor, MDL28170. Six hours later, rings were washed and pre-contracted with U46619 (30 nmol/l). Vasodilation responses were determined through the addition of 0.01 to 100 µM acetylcholine (ACh) or 0.0001 to 1 µM sodium nitroprusside (SNP), as described previously [23].

## Western blot analysis

Total proteins were analysed by SDS-PAGE and blotted using standard protocols [24]. Densitometric quantification was performed with Quantity One software (Bio-Rad). Protein levels (arbitrary units) were normalized to β-actin and expressed as percentage of control values.

## Statistics

All values are expressed as mean ± standard deviation, unless noted otherwise. Endothelium-dependent relaxation was analysed using a two-way ANOVA, followed by multiple t-tests. All other results were analysed using the Student's t-test. The value  $P < 0.05$  was considered significant.

## Results

### HOG-LDL, but not N-LDL, suppresses the production of nitric oxide

Because nitric oxide is a key factor for maintaining vascular homeostasis, we tested the effect of HOG-LDL on nitric oxide production in BAECs. Confluent BAECs were exposed to HOG-LDL at a concentration of 100 µg/ml, which is considered to be pathologically relevant to type 2 diabetes [25]. A 6-hr exposure to HOG-LDL

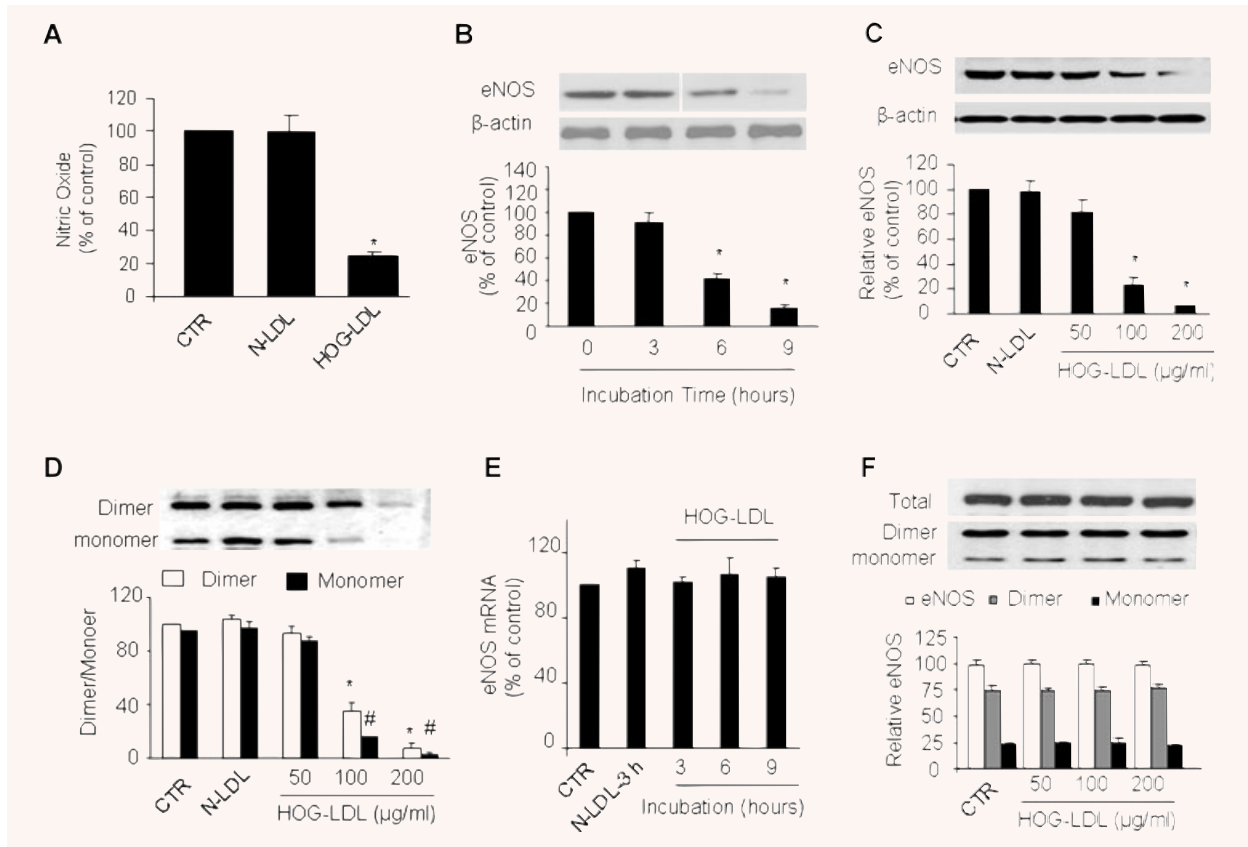


**Fig. 1** HOG-LDL reduces nitric oxide and eNOS levels in endothelial cells. **(A)** Nitric oxide release in BAECs exposed to HOG-LDL or N-LDL (100  $\mu\text{g/ml}$ ) for 6 hrs  $n = 4$ ,  $*P < 0.01$  versus control or N-LDL. **(B)** Western blot analysis of total eNOS in BAECs exposed to HOG-LDL (100  $\mu\text{g/ml}$ ) for the indicated times.  $n = 3$ ,  $**P < 0.01$  versus 0 or 3 hrs time-point. **(C)** Concentration-dependent effects of HOG-LDL on total eNOS protein levels in BAECs.  $n = 4$ ,  $**P < 0.01$  versus untreated control or N-LDL (100  $\mu\text{g/ml}$ ). **(D)** Western blot analysis of dimeric and monomeric eNOS in BAECs exposed to N-LDL or the indicated concentration of HOG-LDL.  $*\#P < 0.01$ . HOG-LDL versus untreated controls or N-LDL. **(E)** Real time qPCR analysis of eNOS in BAECs treated with 100  $\mu\text{g/ml}$  N-LDL or HOG-LDL. PCR was performed with three pairs of independent eNOS primers,  $n = 3$  for each group. **(F)** Effect of increasing concentrations of HOG-LDL on recombinant eNOS protein levels (total, monomeric and dimeric). HOG-LDL was incubated with recombinant eNOS for 6 hrs,  $n = 6$  for each group.

decreased nitric oxide levels by 78%, whereas N-LDL had no effect (Fig. 1A).

### HOG-LDL, but not N-LDL, elicits a dose- and time-dependent reduction in eNOS

Next, we investigated whether HOG-LDL reduces nitric oxide production in BAECs by lowering total eNOS protein levels. No appreciable change in total eNOS protein levels was observed at 3 hrs of HOG-LDL (100  $\mu\text{g/ml}$ ) incubation; however, total eNOS levels were progressively decreased by 60% at 6 hrs and 80% at 9 hrs after incubation (Fig. 1B).

The effects of HOG-LDL were also dose-dependent. As shown in Fig. 1C, a 6-hr incubation with 100  $\mu\text{g/ml}$  or 200  $\mu\text{g/ml}$  HOG-

LDL reduced total eNOS levels by 60% and 80%, respectively. Because the zinc-thiolate cluster of eNOS is essential for eNOS activity and eNOS is active only as a dimer, we investigated whether HOG-LDL may selectively decrease levels of eNOS dimers. A 6-hr exposure to HOG-LDL (100 or 200  $\mu\text{g/ml}$ ), but not N-LDL, reduced the levels of eNOS dimers and monomers to a similar degree (Fig. 1D).

### HOG-LDL does not alter eNOS transcription or directly degrade eNOS

To determine if reduction of eNOS protein levels by HOG-LDL was due to inhibition of eNOS transcription, we tested the effect of HOG-LDL treatment on eNOS mRNA levels in BAECs. Real time

PCR revealed that HOG-LDL exposure did not alter eNOS mRNA levels (Fig. 1E), implying that HOG-LDL does not reduce eNOS protein levels through inhibition of eNOS transcription.

Next, we investigated whether HOG-LDL reduces eNOS protein in BAECs by direct oxidation of eNOS. To this end, purified recombinant bovine eNOS was incubated with HOG-LDL (50, 100 or 200  $\mu\text{g/ml}$ ) for up to 6 hrs. Exposure of recombinant eNOS to HOG-LDL (up to 200  $\mu\text{g/ml}$ ) for 6 hrs did not alter the levels of total eNOS, eNOS dimers or eNOS monomers (Fig. 1F). This suggests that eNOS reduction cannot be attributed to direct destruction or fragmentation of eNOS by HOG-LDL.

### HOG-LDL-enhanced eNOS reduction is independent of 26S proteasomes

Because HOG-LDL did not alter eNOS levels in a cell-free system and eNOS reduction in BAECs required at least a 3-hr incubation with HOG-LDL, we speculated that HOG-LDL might reduce eNOS levels by inducing eNOS degradation. Studies [26, 27] suggest that eNOS is degraded by several mechanisms, including those involving 26S proteasomes and calcium-dependent calpain. As shown in Fig. 2A, exposure of BAECs to HOG-LDL (100  $\mu\text{g/ml}$  for 6 hrs) did not alter 26S proteasome activity. In addition, neither HOG-LDL nor N-LDL affected the levels of protein ubiquitination (Fig. 2B). Furthermore, eNOS reduction by HOG-LDL was unaffected by co-administration of MG132, a potent proteasome inhibitor (Fig. 2C). Taken together, these results suggest that HOG-LDL-induced reduction in eNOS occurs independently of 26S proteasomes.

### HOG-LDL increases calpain activity and eNOS translocation to the cytoplasm, where calpains reside

Calpains are  $\text{Ca}^{2+}$ -dependent cysteine proteases which are implicated in a large number of physiological processes [28, 29]. Calpain activity assays revealed that HOG-LDL markedly increased the calpain activity in BAECs (Fig. 2D). Exposure of BAECs to HOG-LDL for 6 hrs led to cleavage of the calpain substrate, caspase-12 [30], confirming that HOG-LDL induces calpain activation (Fig. 2E).

If eNOS is degraded by calpain, then a physical association between these two proteins would be required. However, eNOS exists predominantly in caveolae of the plasma membrane [31], whereas calpains exist mainly in cytoplasm. Thus, we investigated whether HOG-LDL alters the subcellular localization of eNOS in BAECs. After 2 hrs treatment, both immunocytochemical staining (Fig. 2F) and Western blot analysis of membrane and cytosolic fractions (Fig. 2G) revealed that HOG-LDL but not n-LDL (control) induced the translocation of eNOS from the plasma membrane to the cytosol, where calpains mainly reside. HOG-LDL also increased levels of Ser1177-phosphorylated eNOS (data not shown).

### Calpain inhibition prevents reduction of eNOS levels by HOG-LDL

As HOG-LDL increased calpain activity and eNOS export to the cytoplasm, we determined if selective pharmacologic or genetic inhibition of calpains attenuated the reduction in eNOS elicited by HOG-LDL in BAECs. Calpain inhibitors alone did not alter the levels of total, dimeric or monomeric eNOS (data not shown). However, treatment of cells with calpain inhibitor III (MDL28170), calpeptin, ALLM, ALLN or E64 prior to HOG-LDL exposure prevented reduction of total, dimeric and monomeric eNOS (Fig. 3A–C). To exclude off-target effects of calpain inhibitors, we tested the effect of genetic calpain inhibition on eNOS reduction by HOG-LDL. As the siRNA against bovine calpain was not available, we performed these experiments on HUVECs, which, like BAECs, express both eNOS and calpain. Transfection of calpain-specific siRNA, but not control siRNA, reduced calpain protein levels by 60% in HUVECs (Fig. 3D). Calpain 1-specific siRNA partially prevented eNOS reduction by HOG-LDL, whereas control siRNA had no effect (Fig. 3D).

### HOG-LDL increases cytosolic $\text{Ca}^{2+}$ levels

Calpain activity is strictly controlled by intracellular  $\text{Ca}^{2+}$ , prompting us to test if calpain activation by HOG-LDL is  $\text{Ca}^{2+}$ -dependent. HOG-LDL ( $>50 \mu\text{g/ml}$ ) induced a pronounced elevation in intracellular  $\text{Ca}^{2+}$  in BAECs, whereas N-LDL (100  $\mu\text{g/ml}$ ) had no effect (Fig. 4A). EGTA or either of the two potent  $\text{Ca}^{2+}$  channel blockers,  $\text{CoCl}_2$  or  $\text{LaCl}_3$ , significantly suppressed HOG-LDL-induced elevation in intracellular  $\text{Ca}^{2+}$  (Fig. 4B). Verapamil, a phenylalkylamine  $\text{Ca}^{2+}$  channel blocker, had a similar effect (Fig. 4B). These results imply that HOG-LDL increases cytosolic  $\text{Ca}^{2+}$  levels by opening  $\text{Ca}^{2+}$  channels.

### Inhibition of HOG-LDL-induced elevation in intracellular $\text{Ca}^{2+}$ prevents eNOS degradation

Next, we investigated the  $\text{Ca}^{2+}$  dependence of HOG-LDL-induced eNOS degradation. Decreasing free intracellular  $\text{Ca}^{2+}$  with 1.0–2.5 mM EGTA abolished eNOS reduction in BAECs exposed to 100  $\mu\text{g/ml}$  HOG-LDL (Fig. 4C). Similarly,  $\text{Ca}^{2+}$ -channel blockers (*i.e.*  $\text{CoCl}_3$ ,  $\text{LaCl}_3$ , verapamil; Fig. 4D) or the intracellular  $\text{Ca}^{2+}$  chelator, BAPTA (Fig. 4E and F), also significantly reversed HOG-LDL-induced eNOS degradation. These results suggest that HOG-LDL promotes eNOS degradation by increasing intracellular  $\text{Ca}^{2+}$  concentrations.

### HOG-LDL increases the formation of ROS and the membrane translocation of the p47<sup>phox</sup> NAD(P)H oxidase subunit

Recent studies by our laboratory and others suggest that ROS cause the vascular injury induced by oxidized LDL (See review

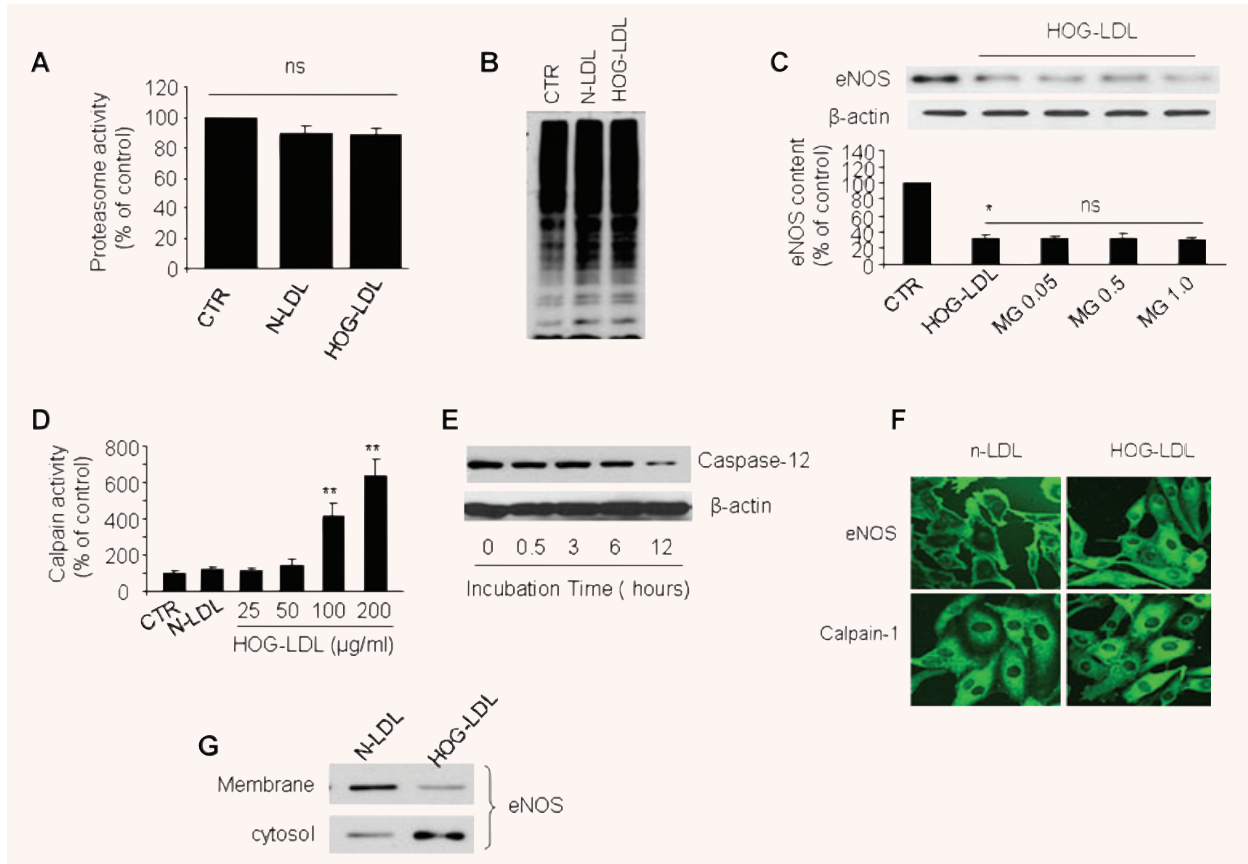


**Fig. 2** HOG-LDL selectively activates calpain and induces cytoplasmic translocation of eNOS (A) Effect of HOG-LDL on 26S proteasome activity in BAECs.  $n = 3$ ; ns, non significant difference for control versus HOG-LDL. (B) Effect of HOG-LDL on protein ubiquitination in BAECs, as determined by Western blot analysis.  $n = 3$  for each group. (C) Western blot analysis of eNOS levels in BAECs exposed to HOG-LDL in the presence or absence of MG132. The blot is a representative of four blots obtained from four separate experiments. \* $P < 0.01$  HOG-LDL versus control; NS, no significant difference. (D) Calpain activity in BAECs treated with N-LDL (100  $\mu\text{g/ml}$ ) or increasing concentrations of HOG-LDL for 6 hrs  $n = 3$ , \*\* $P < 0.01$  versus untreated controls or n-LDL. (E) Effect of HOG-LDL on caspase 12 cleavage. The blot is representative of three separate experiments. (F) Confocal images (400 $\times$ ) of eNOS immunofluorescent staining in control and HOG-LDL-treated BAECs. Note the redistribution of eNOS from the plasma membrane to the cytoplasm in the presence of HOG-LDL. (G) Western blot analysis for eNOS in membrane and cytosolic fractions isolated from control or HOG-LDL-treated BAECs.  $n = 3$  for both groups.

[32]). Thus, we hypothesized that ROS mediate the elevation in intracellular  $\text{Ca}^{2+}$  and subsequent calpain activation by HOG-LDL. In accordance with this hypothesis, HOG-LDL increased  $\text{O}_2^-$  levels by  $\sim 4$ -fold ( $P < 0.01$ ), whereas N-LDL had no effect (Fig. 5A). In addition,  $\text{H}_2\text{O}_2$  was increased approximately twofold following 6 hrs of HOG-LDL treatment (Fig. 5B).

The formation of  $\text{O}_2^-$  in HOG-LDL-exposed BAECs was significantly suppressed by inhibition of NAD(P)H oxidase with apocynin (data not shown), suggesting that NAD(P)H oxidase may contribute to HOG-LDL-induced oxidative stress. Western blot analysis of subcellular fractions revealed that HOG-LDL induced p47<sup>phox</sup> translocation from the cytosol to the plasma membrane (Fig. 5C), a signature of NAD(P)H oxidase activation [33]. The

p47<sup>phox</sup> membrane translocation was not seen in N-LDL-treated BAECs. These results suggest that HOG-LDL activates NAD(P)H oxidase, consistent with a previous report [34].

### Inhibition of ROS formation attenuates HOG-LDL-induced elevation in intracellular $\text{Ca}^{2+}$

Blocking  $\text{Ca}^{2+}$  influx with EGTA in HOG-LDL-treated BAECs not only prevented eNOS degradation, but also dramatically reduced  $\text{O}_2^-$  and  $\text{H}_2\text{O}_2$  production (Fig. 5D and E). Accordingly, inhibition of NAD(P)H oxidase activity with apocynin or DPI attenuated increases in intracellular  $\text{Ca}^{2+}$  (Fig. 5F) as well as eNOS degradation

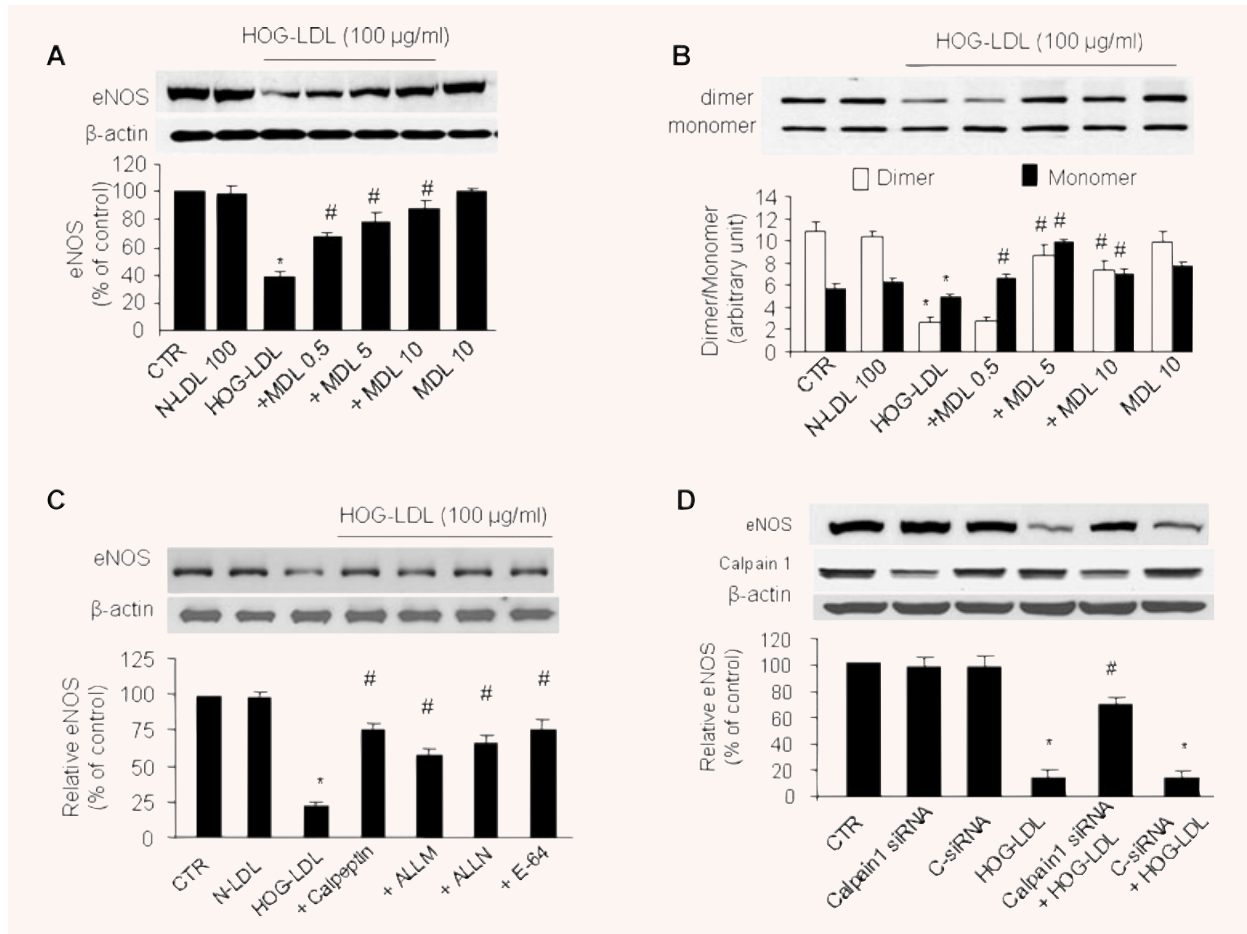


**Fig. 3** Pharmacological or genetic inhibition of calpain prevents reduction of eNOS by HOG-LDL. Western blot analysis of (A) total eNOS as well as (B) dimeric and monomeric eNOS in BAECs exposed to HOG-LDL in the presence or absence of the indicated concentration of the calpain inhibitor III, MDL28170. *n* = 3, \**P* < 0.01 versus control, #*P* < 0.01 versus HOG-LDL-treated groups. (C) Effect of the other calpain inhibitors, calpeptin (20 μM), ALLM (20 μM), ALLN (20 μM) or E-64 (15 μM), on total eNOS levels in HOG-LDL-exposed BAECs. \**P* < 0.01 versus untreated controls or n-LDL, #*P* < 0.01 versus HOG-LDL. (D) Western blot analysis of eNOS, and calpain 1 in HOG-LDL-stimulated HUVECs transfected with calpain 1 siRNA or scrambled siRNA for 48 hrs. \**P* < 0.01 versus control, #*P* < 0.01 versus HOG-LDL. The blot is a representative of four blots obtained from four separate experiments.

in HOG-LDL-treated BAECs (Fig. 5G). Taken together, these results suggest that exposure of endothelial cells to HOG-LDL triggers production of ROS that, in turn, induce Ca<sup>2+</sup> influx into the cytoplasm to stimulate calpain-dependent eNOS degradation.

### HOG-LDL reduces aortic eNOS levels and impairs endothelial function in a calpain-dependent manner

Next, we determined whether HOG-LDL induces calpain-dependent eNOS degradation in intact aortas. Isolated mouse aortas were exposed to either N-LDL or HOG-LDL in the presence or absence

of MDL28170, and eNOS protein levels were measured. Exposure of mouse aortas to MDL28170 alone (data not shown) or N-LDL (Fig. 6A) did not affect eNOS levels. In contrast, exposure of aortas to 100 μg/ml HOG-LDL for 24 hrs reduced eNOS protein levels by 75–80% (*P* < 0.05, Fig. 6A). Importantly, this reduction in aortic eNOS levels was almost completely blocked by co-administration of MDL28170 (Fig. 6A).

To investigate the role of HOG-LDL-induced calpain activation in endothelial dysfunction, we tested the effect of N-LDL, HOG-LDL and HOG-LDL + MDL28170 on endothelium-dependent and -independent vasorelaxation under *ex vivo* conditions. Acetylcholine induced concentration-dependent arterial vasodilatation in all treatment groups (Fig. 6B). MDL28170 alone has no effect on vasorelaxation. However, Ach-induced vasodilatation

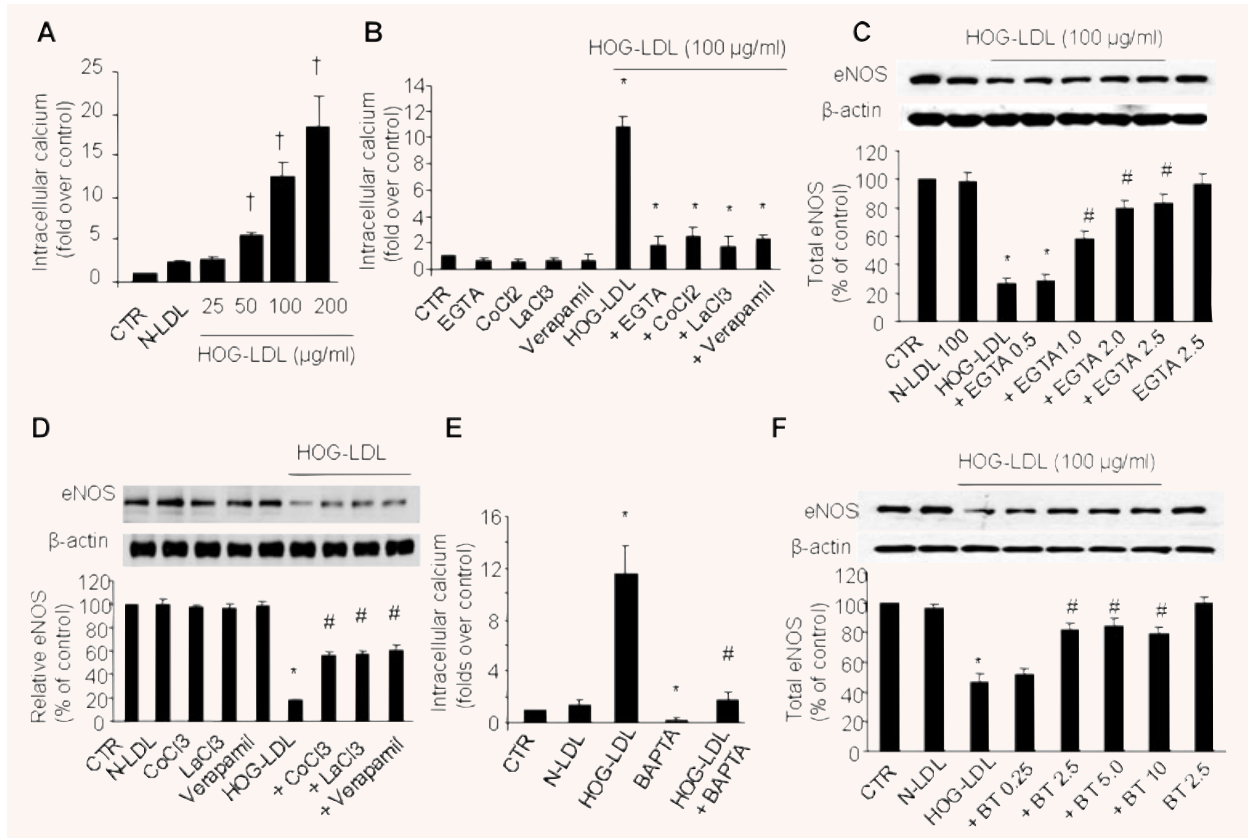


**Fig. 4** HOG-LDL increases intracellular  $\text{Ca}^{2+}$ , and chelation of  $\text{Ca}^{2+}$  protects eNOS from degradation. **(A)** Intracellular  $\text{Ca}^{2+}$  concentrations in BAECs exposed to HOG-LDL (100  $\mu\text{g}/\text{ml}$ ) for 6 hrs,  $n = 4$ ,  $^{++}P < 0.01$  versus untreated controls or n-LDL. **(B)** Effect of the  $\text{Ca}^{2+}$  channel blockers,  $\text{CoCl}_2$  (1 mM),  $\text{LaCl}_3$  (0.2 mM) or verapamil (1 mM), on HOG-LDL-induced  $\text{Ca}^{2+}$  influx.  $n = 3$ ,  $^{**}P < 0.01$  versus HOG-LDL. **(C)** Effect of EGTA (0.5–2.5 mM) on HOG-LDL-induced reduction in total eNOS protein levels.  $n = 3$ ,  $^{*}P < 0.01$  versus control,  $^{\#}P < 0.01$  versus HOG-LDL. **(D)** Effect of the  $\text{Ca}^{2+}$  channel blockers,  $\text{CoCl}_3$  (1 mM),  $\text{LaCl}_3$  (0.2 mM) or verapamil (1 mM), on total eNOS levels in HOG-LDL-treated BAECs.  $n = 4$ ,  $^{*}P < 0.01$  versus untreated controls or n-LDL,  $^{\#}P < 0.01$  versus HOG-LDL. **(E)** Intracellular  $\text{Ca}^{2+}$  levels in BAECs exposed to HOG-LDL for 6 hrs in the presence or absence of the  $\text{Ca}^{2+}$  chelator, 5  $\mu\text{M}$  of BAPT-AM (30-min. pre-incubation).  $n = 4$ ,  $^{*}P < 0.01$  versus control,  $^{\#}P < 0.01$  versus HOG-LDL. **(F)** Effect of BAPT-AM (0.25–10  $\mu\text{M}$ ) on total eNOS levels in HOG-LDL-exposed BAECs.  $n = 4$ ,  $^{*}P < 0.01$  versus control,  $^{\#}P < 0.01$  versus HOG-LDL.

was markedly attenuated in HOG-LDL-treated aortas compared to N-LDL-treated aortas, with the maximum arterial relaxation response in the HOG-LDL group being  $42.2 \pm 4.6\%$  and that in the N-LDL group being  $88.6 \pm 8.5\%$  ( $n = 4$  per group,  $P < 0.01$ ). Further, MDL28170 significantly improved Ach-induced vasodilation in the aortas treated with HOG-LDL. In contrast to Ach-induced endothelium-dependent relaxation, SNP-induced endothelium-independent vasorelaxation was identical among all groups (Fig. 6C). Together, these data suggest that calpain participates in HOG-LDL-induced endothelial dysfunction.

## Discussion

Nitric oxide from eNOS plays essential role in maintaining vascular homeostasis [35]. Reduced nitric oxide generation and/or

bioavailability have been implicated in the pathophysiology of several disease states including coronary artery disease, hypertension, diabetes and heart failure [36, 37]. eNOS is regulated at the transcriptional, post-transcriptional and post-translational level. Earlier studies suggest that increased intracellular  $\text{Ca}^{2+}$  and eNOS phosphorylation induce a rapid and transient elevation in eNOS activity, allowing for fast responses to changing environmental conditions [38, 39]. Sustained alterations are primarily due to changes in the expression of eNOS protein [40]. In the present study, we have provided convincing evidence that HOG-LDL perturbs intracellular  $\text{Ca}^{2+}$  homeostasis, resulting in calpain-dependent degradation of eNOS and consequent endothelial dysfunction. Our study strongly suggests that HOG-LDL-induced eNOS degradation was associated with endothelial dysfunction.

The calpains are a family of calcium-dependent proteases that act independently of the proteasome pathway and cleave



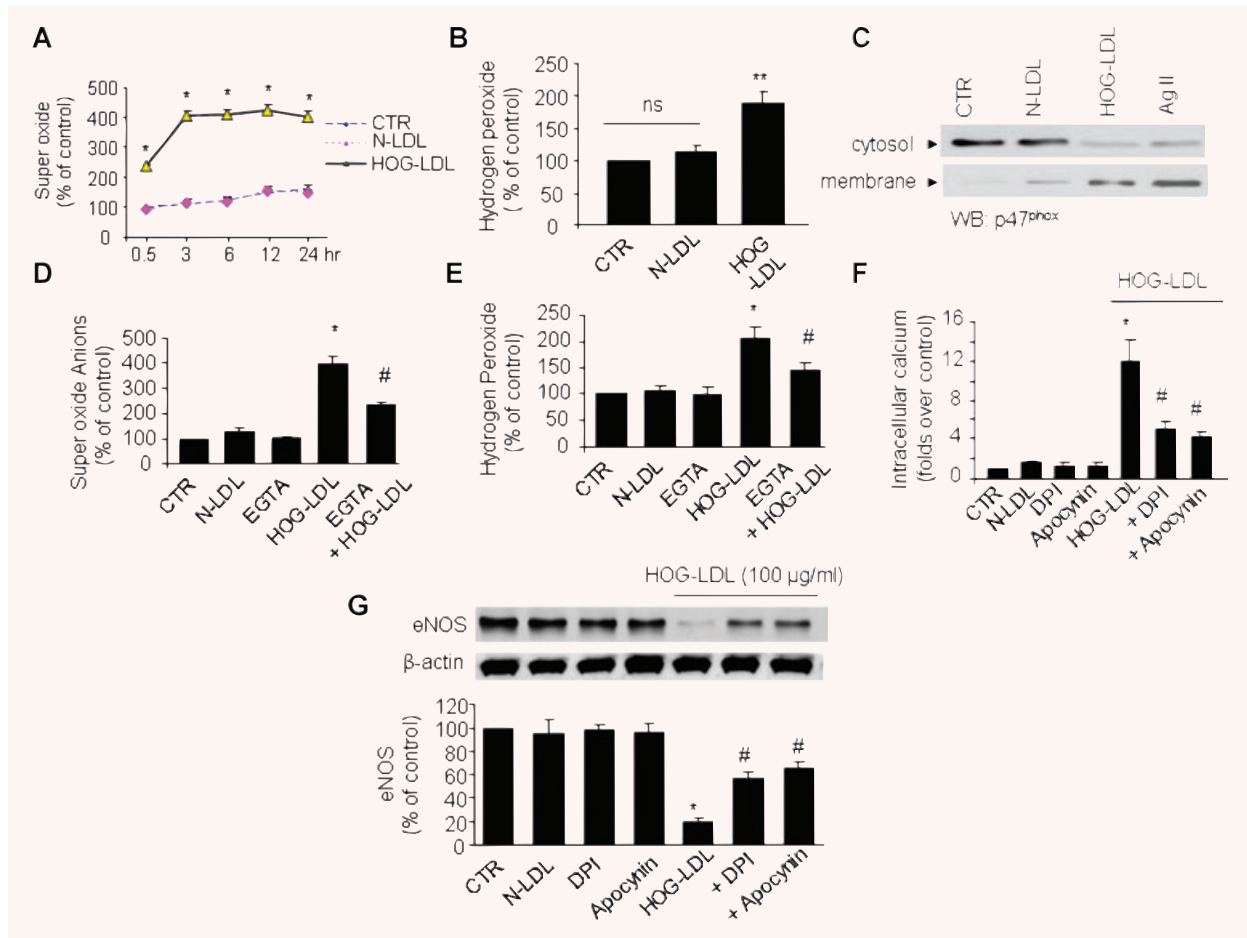


**Fig. 5** HOG-LDL-induced increases in intracellular  $\text{Ca}^{2+}$  and decreases in eNOS are ROS-dependent. **(A)** Superoxide ( $\text{O}_2^-$ ) production in BAECs exposed to HOG-LDL (100  $\mu\text{g}/\text{ml}$ , time course).  $n = 4$ ,  $*P < 0.01$  Controls versus each time-point. **(B)** Hydrogen peroxide ( $\text{H}_2\text{O}_2$ ) production in HOG-LDL-exposed BAECs.  $n = 4$ ,  $**P < 0.01$  versus control. **(C)** Effect of HOG-LDL on NADPH oxidase activation, as determined by membrane translocation of p47<sup>phox</sup>. BAECs exposed to agentension II (Ang II, 1  $\mu\text{M}$ ) served as a positive control. The Western blot shown is representative of four blots obtained from four separate experiments. **(D)** Effect of EGTA (2.5 mM, 1-hr pre-incubation) on HOG-LDL-induced  $\text{O}_2^-$  release in BAECs.  $n = 3$ ,  $**P < 0.01$  versus control,  $##P < 0.01$  versus HOG-LDL. **(E)**  $\text{H}_2\text{O}_2$  production in BAECs treated with HOG-LDL  $\pm$  EGTA.  $n = 3$ ,  $*P < 0.05$  versus control,  $#P < 0.05$  versus HOG-LDL. **(F)** Effect of apocynin (100  $\mu\text{M}$ ) or DPI (10  $\mu\text{M}$ ) on intracellular  $\text{Ca}^{2+}$  levels in BAEC exposed to HOG-LDL.  $n = 3$ ,  $**P < 0.01$  versus control,  $##P < 0.01$  versus HOG-LDL. **(G)** Effect of apocynin or DPI on eNOS degradation by HOG-LDL (100  $\mu\text{g}/\text{ml}$ , 6 hrs),  $n = 4$ ,  $*P < 0.01$  versus untreated controls or n-LDL,  $#P < 0.01$  versus HOG-LDL.

a number of cellular substrates, including kinases, phosphatases, transcription factors and cytoskeletal proteins. The calpains are a family of  $\text{Ca}^{2+}$ -dependent cysteine proteases, which comprises three molecules:  $\mu$ -calpain (calpain1), m-calpain and calpastatin, a third polypeptide functioning as an inhibitor for two calpains. The  $\mu$ -calpain is activated by micromolar concentrations of  $\text{Ca}^{2+}$  whereas m-calpain activation requires millimolar concentrations of  $\text{Ca}^{2+}$  [41]. One mechanism that may explain the relationship between inhibition of calpain activity and preservation of endothelial nitric

oxide in HOG-LDL treatment is altered post-translational regulation of endothelial nitric oxide synthase. The evidence can be summarized as follows. First, at doses over 50  $\mu\text{g}/\text{ml}$ , HOG-LDL greatly elevated endothelial intracellular  $\text{Ca}^{2+}$ . Second, blockage of  $\text{Ca}^{2+}$  channels and chelation of intracellular  $\text{Ca}^{2+}$  protected eNOS from HOG-LDL-induced degradation. Third, HOG-LDL increased calpain activity. Fourth, genetic inhibition of calpain abolished HOG-LDL-induced eNOS degradation. Finally, calpain inhibition restored Ach-induced endothelium-dependent relaxation in isolated mouse aortas. In agreement

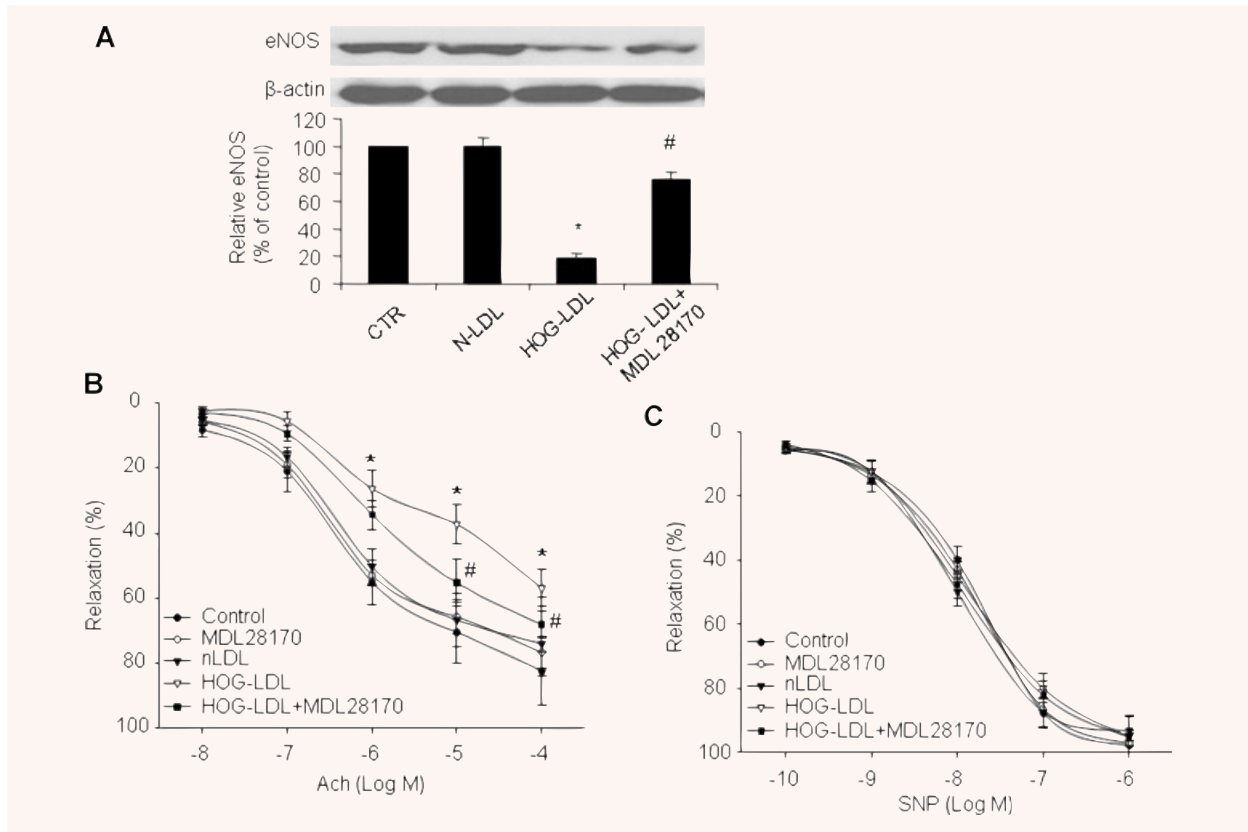


**Fig. 6** HOG-LDL-induced activation of calpain decreases eNOS levels and impairs endothelium-dependent relaxation in C57BL/6J mice aorta. **(A)** Western blot analysis of total eNOS levels in aortas incubated with HOG-LDL (100  $\mu$ g/ml for 24 hrs) in the presence or absence of the calpain inhibitor III, MDL28170 (20  $\mu$ M).  $n = 4$  in each group, \*\* $P < 0.01$  versus N-LDL, \*\* $P < 0.01$  versus HOG-LDL. **(B)** Endothelium-dependent relaxation of HOG-LDL-exposed aortas treated with or without MDL28170.  $n = 5$ , \* $P < 0.05$  for HOG-LDL versus untreated control or N-LDL, # $P < 0.05$  for HOG-LDL versus HOG-LDL + MDL28170. **(C)** Endothelium-independent relaxation in aortas treated with HOG-LDL  $\pm$  MDL28170. Results (mean  $\pm$  S.E.M.) are expressed as the rate of relaxation to the pre-contraction,  $n = 4$ .

with our findings, several studies have demonstrated that pharmacological inhibition of calpain preserves eNOS function [42] and that calpain impairs association between eNOS and the regulatory protein heat shock protein 90 [26], which is also a calpain substrate [43]. Calpain 10 has recently been linked to diabetes [44]. In addition, platelets from type 2 diabetic patients contain elevated  $Ca^{2+}$  and  $\mu$ -calpain activity [45]. Thus, preservation of endothelial nitric oxide availability could account for the beneficial effects of calpain inhibition on HOG-LDL-induced vascular impairment. As levels of glycated and oxidized LDL are elevated in patients with diabetes, these findings might help uncover novel signalling pathways accelerating atherosclerosis in these patients.

In conclusion, we have demonstrated that  $[Ca^{2+}]_i$  and calpain activity are increased in endothelial cells in response to HOG-LDL, and that inhibition of  $[Ca^{2+}]_i$  rise and calpain activity attenuates

endothelial dysfunction induced by HOG-LDL via a eNOS/nitric oxide dependent mechanism. Our findings uncovered a novel signalling pathway implicated in the pathophysiology of diabetic vascular diseases such as atherosclerosis.

## Acknowledgements

This work was supported by grants from the NIH (HL079584, HL074399, HL080499 and HL089920), the American Diabetes Association, the Juvenile Diabetes Research Foundation and the Oklahoma Center for Advancement of Science and Technology (OCAST). It was also supported by funds from the Travis Endowed Chair in Endocrinology, University of Oklahoma Health Sciences Center (all to M.H.Z.) and grants from the NIH (HL55782 and HL80921) and the American Diabetes Association (1-05-RA-74) to T.J.L.

## References

1. **Chapman MJ.** Metabolic syndrome and type 2 diabetes: lipid and physiological consequences. *Diab Vasc Dis Res.* 2007; 4: 5–8.
2. **Lyons TJ, Jenkins AJ.** Glycation, oxidation and lipoxidation in the development of the complications of diabetes mellitus: a “carbonyl stress” hypothesis. *Diabetes Rev.* 1997; 5: 365–91.
3. **Tsimikas S, Glass C, Steinberg D.** Lipoproteins, lipoprotein oxidation and atherogenesis. In: Chien KR, editor. *Molecular basis of cardiovascular disease: a companion to Braunwald’s heart disease.* Philadelphia: W.B. Saunders Company; 2004. pp. 385–413.
4. **Brownlee M.** Advanced protein glycosylation in diabetes and aging. *Annu Rev Med.* 1995; 46: 223–34.
5. **Kennedy AL, Lyons TJ.** Glycation, oxidation, and lipoxidation in the development of diabetic complications. *Metabolism.* 1997; 46: 14–21.
6. **Gugliucci Creriche A, Dumont S, Siffert JC, et al.** *In vitro* glycated low-density lipoprotein interaction with human monocyte-derived macrophages. *Res Immunol.* 1992; 143: 17–23.
7. **Kobayashi K, Watanabe J, Umeda F, et al.** Glycation accelerates the oxidation of low density lipoprotein by copper ions. *Endocr J.* 1995; 42: 461–5.
8. **Millican SA, Schultz D, Bagga M, et al.** Glucose-modified low density lipoprotein enhances human monocyte chemotaxis. *Free Radic Res.* 1998; 28: 533–42.
9. **Forstermann U, Munzel T.** Endothelial nitric oxide synthase in vascular disease: from marvel to menace. *Circulation.* 2006; 113: 1708–14.
10. **Forstermann U, Closs EI, Pollock JS, et al.** Nitric oxide synthase isozymes. Characterization, purification, molecular cloning, and functions. *Hypertension.* 1994; 23: 1121–31.
11. **Kawashima S, Yokoyama M.** Dysfunction of endothelial nitric oxide synthase and atherosclerosis. *Arterioscler Thromb Vasc Biol.* 2004; 24: 998–1005.
12. **Zou MH, Cohen R, Ullrich V.** Peroxynitrite and vascular endothelial dysfunction in diabetes mellitus. *Endothelium.* 2004; 11: 89–97.
13. **Zou MH.** Peroxynitrite and protein tyrosine nitration of prostacyclin synthase. *Prostaglandins Other Lipid Mediat.* 2007; 82: 119–27.
14. **Navab M, Ananthramaiah GM, Reddy ST, et al.** The oxidation hypothesis of atherogenesis: the role of oxidized phospholipids and HDL. *J Lipid Res.* 2004; 45: 993–1007.
15. **Matsumoto T, Takashima H, Ohira N, et al.** Plasma level of oxidized low-density lipoprotein is an independent determinant of coronary macrovasomotor and microvasomotor responses induced by bradykinin. *J Am Coll Cardiol.* 2004; 44: 451–7.
16. **Fraley AE, Tsimikas S.** Clinical applications of circulating oxidized low-density lipoprotein biomarkers in cardiovascular disease. *Curr Opin Lipidol.* 2006; 17: 502–9.
17. **Jenkins AJ, Velarde V, Klein RL, et al.** Native and modified LDL activate extracellular signal-regulated kinases in mesangial cells. *Diabetes* 2000; 49: 2160–9.
18. **Xu J, Xie Z, Reece R, et al.** Uncoupling of endothelial nitric oxidase synthase by hypochlorous acid: role of NAD(P)H oxidase-derived superoxide and peroxynitrite. *Arterioscler Thromb Vasc Biol.* 2006; 26: 2688–95.
19. **Xie Z, Dong Y, Scholz R, et al.** Phosphorylation of LKB1 at serine 428 by protein kinase C-zeta is required for metformin-enhanced activation of the AMP-activated protein kinase in endothelial cells. *Circulation.* 2008; 117: 952–62.
20. **Zhang M, Dong Y, Xu J, et al.** Thromboxane receptor activates the AMP-activated protein kinase in vascular smooth muscle cells via hydrogen peroxide. *Circ Res.* 2008; 102: 328–37.
21. **Pfaffl MW.** A new mathematical model for relative quantification in real-time RT-PCR. *Nucleic Acids Res.* 2001; 29: e45.
22. **Dong Y, Tan J, Cui MZ, et al.** Calpain inhibitor MDL28170 modulates Abeta formation by inhibiting the formation of intermediate Abeta46 and protecting Abeta from degradation. *FASEB J.* 2006; 20: 331–3.
23. **Xu J, Wu Y, Song P, et al.** Proteasome-dependent degradation of guanosine 5′-triphosphate cyclohydrolase I causes tetrahydrobiopterin deficiency in diabetes mellitus. *Circulation.* 2007; 116: 944–53.
24. **Xie Z, Dong Y, Zhang M, et al.** Activation of protein kinase C zeta by peroxynitrite regulates LKB1-dependent AMP-activated protein kinase in cultured endothelial cells. *J Biol Chem.* 2006; 281: 6366–75.
25. **Klein RL, Semler AJ, Baynes JW, et al.** Glycation does not alter LDL-induced secretion of tissue plasminogen activator and plasminogen activator inhibitor-1 from human aortic endothelial cells. *Ann N Y Acad Sci.* 2005; 1043: 379–89.
26. **Stalker TJ, Gong Y, Scalia R.** The calcium-dependent protease calpain causes endothelial dysfunction in type 2 diabetes. *Diabetes.* 2005; 54: 1132–40.
27. **Jiang J, Cyr D, Babbitt RW, et al.** Chaperone-dependent regulation of endothelial nitric-oxide synthase intracellular trafficking by the co-chaperone/ubiquitin ligase CHIP. *J Biol Chem.* 2003; 278: 49332–41.
28. **Johnson GV, Guttman RP.** Calpains: intact and active? *Bioessays.* 1997; 19: 1011–8.
29. **Huang Y, Wang KK.** The calpain family and human disease. *Trends Mol Med.* 2001; 7: 355–62.
30. **Nakagawa T, Yuan J.** Cross-talk between two cysteine protease families. Activation of caspase-12 by calpain in apoptosis. *J Cell Biol.* 2000; 150: 887–94.
31. **Minshall RD, Sessa WC, Stan RV, et al.** Caveolin regulation of endothelial function. *Am J Physiol Lung Cell Mol Physiol.* 2003; 285: 1179–83.
32. **Chen K, Thomas SR, Keane JF Jr.** Beyond LDL oxidation: ROS in vascular signal transduction. *Free Radic Biol Med.* 2003; 35: 117–32.
33. **Li JM, Mullen AM, Yun S, et al.** Essential role of the NADPH oxidase subunit p47(phox) in endothelial cell superoxide production in response to phorbol ester and tumor necrosis factor-alpha. *Circ Res.* 2002; 90: 143–50.
34. **O’Donnell RW, Johnson DK, Ziegler LM, et al.** Endothelial NADPH oxidase: mechanism of activation by low-density lipoprotein. *Endothelium.* 2003; 10: 291–7.
35. **Stangl V, Lorenz M, Meiners S, et al.** Long-term up-regulation of eNOS and improvement of endothelial function by inhibition of the ubiquitin-proteasome pathway. *FASEB J.* 2004; 18: 272–9.
36. **Kojda G, Harrison D.** Interactions between NO and reactive oxygen species: pathophysiological importance in atherosclerosis, hypertension, diabetes and heart failure. *Cardiovasc Res.* 1999; 43: 562–71.
37. **Demar BS, Tschudi MR, Godoy N, et al.** Reduced endothelial nitric oxide synthase expression and production in human

- atherosclerosis. *Circulation*. 1998; 97: 2494–8.
38. **Dimmeler S, Fleming I, Fisslthaler B, et al.** Activation of nitric oxide synthase in endothelial cells by Akt-dependent phosphorylation. *Nature*. 1999; 399: 601–5.
  39. **Dimmeler S, Dernbach E, Zeiher AM.** Phosphorylation of the endothelial nitric oxide synthase at ser-1177 is required for VEGF-induced endothelial cell migration. *FEBS Lett*. 2000; 477: 258–62.
  40. **Wu KK.** Regulation of endothelial nitric oxide synthase activity and gene expression. *Ann N Y Acad Sci*. 2002; 962: 122–30.
  41. **Goll DE, Thompson VF, Li H, et al.** The calpain system. *Physiol Rev*. 2003; 83: 731–801.
  42. **Stalker TJ, Skvarka CB, Scalia R.** A novel role for calpains in the endothelial dysfunction of hyperglycemia. *FASEB J*. 2003; 17: 1511–3.
  43. **Su Y, Block ER.** Role of calpain in hypoxic inhibition of nitric oxide synthase activity in pulmonary endothelial cells. *Am J Physiol Lung Cell Mol Physiol*. 2000; 278: 1204–12.
  44. **Horikawa Y, Oda N, Cox NJ, et al.** Genetic variation in the gene encoding calpain-10 is associated with type 2 diabetes mellitus. *Nat Genet*. 2000; 26: 163–75.
  45. **Randriamboavonjy V, Pistrosch F, Bolck B, et al.** Platelet sarcoplasmic endoplasmic reticulum Ca<sup>2+</sup>-ATPase and mu-calpain activity are altered in type 2 diabetes mellitus and restored by rosiglitazone. *Circulation*. 2008; 117: 52–60.